Civil Engineering and Applied Solutions

Research Article

journal homepage: ceas.journals.umz.ac.ir

CEAS Civil Engineering and Applied Solutions

Assessment of the Impact of Land Use/Land Cover Changes in the Hamoun Wetland on Land Surface Temperature Using Satellite Imagery

Mozhgan Yarahmadi [a], Hadi Eskandari Damaneh [b], Shahram Khalighi Sigaroodi [a*]

[a] *Department of Arid and Mountainous Regions Reclamation, Faculty of Natural Resources, University of Tehran, Iran*

[b] *Department of Desert Studies, Research Institute of Forests and Rangelands, Agricultural Research, Education and Extension Organization (AREEO), Tehran, Iran*

ARTICLE INFO

Keywords:
Land use/land cover (LULC) changes
Temperature
Palmer drought severity index (PDSI)
Hamoun

Article history:
Received 7 May 2025
Accepted 26 May 2025
Available online 01 July 2025

ABSTRACT

The Hamoun wetland, situated in southeastern Iran near the Afghanistan border, is a sensitive ecological and socio-economic area that has undergone significant land use and environmental changes over recent decades. This study applied the supervised CART classification method to identify Land Use/Land Cover (LULC) changes over 40 years (corresponding to 1990, 2000, 2010, and 2020) in the Hamoun region. Surface temperature data were analyzed regarding land use changes, and the Palmer Drought Severity Index (PDSI) was utilized to assess drought trends during this time. The results indicate a significant decline in water bodies, agricultural lands, and reed beds. Specifically, the water bodies decreased from 11.25% in 1990 to 2.47% in 2020, agricultural lands from 8.56% to 3.53%, and reed beds from 4.64% to 0.38%. Conversely, low-vegetation areas, barren lands, and urban areas expanded, with barren lands increasing by 14.05%. The overall classification accuracy for the LULC maps was approximately 96%, 96%, 95%, and 98% for the respective years, and the Kappa coefficients were 0.97, 0.97, 0.96, and 0.98, indicating high classification accuracy. Temperature trends declined during the study period, primarily due to severe droughts. The findings highlight a significant relationship between land use changes and surface temperature variations. This research provides valuable insights for policymakers and urban planners, supporting sustainable LULC strategies at the local level.

1. Introduction

Land Use and Land Cover (LULC) changes play a significant role in global and regional climate pattern alterations, including rainfall variability and increases in Land Surface Temperature (LST) [1-4]. Human activities have extensively modified land surface utilization over the past centuries, significantly impacting terrestrial ecosystems and, consequently, the environment [5]. Rapid urbanization and population growth in urban centers are among the primary drivers of land use change. One of the major environmental issues observed across various regions is the rise in LST in response to land use transformations. LST is a critical variable that can be accurately measured using thermal infrared bands with high spatial resolution [6-9]. Therefore, identifying current LULC changes is essential for assessing variations in land surface temperature.

Zhao et al. [10] investigated changes in land use and LULC, land surface temperature (LST), the Normalized Difference Vegetation Index (NDVI), and the Normalized Difference Built-up Index (NDBI) in the Kasur region over three decades. Their findings revealed an expansion of urban areas and a decline in vegetation, water bodies, forests, and barren land, with a negative correlation between NDVI and NDBI. Similarly, Saleem et al. [11] examined LULC changes in the Jammu region of India between

* Corresponding author.
E-mail addresses: Khalighi@ut.ac.ir (S. Khalighi Sigaroodi).

https:// doi.org/10.22080/ceas.2025.29153.1009
ISSN: 3092-7749/
How to cite this article: Yarahmadi, M., Eskandari Damaneh, H., Khalighi Sigaroodi, S. Assessment of the impact of land use/land cover changes in the Hamoun Wetland on land surface temperature using satellite imagery. Civil Engineering and Applied Solutions. 2025; 1(2): 31–42. doi:10.22080/ceas.2025.29153.1009.

1990 and 2020 using remote sensing data, indicating increased agricultural, barren, and settlement areas alongside vegetation loss and rising LST due to climate change. NDVI was highlighted as an effective indicator of vegetation health and its impact on surface temperature. Hussainet al. [12] analyzed LULC changes and their effect on LST in Khanewal, Pakistan, using remote sensing techniques. Their results demonstrated that the rapid expansion of built-up areas led to vegetation decline and temperature rise, primarily driven by population growth, urban development, and infrastructure expansion—findings that are valuable for regional planning and agricultural management. Moreover, Al Rakib et al. [13] studied the effects of rapid urban growth on LULC and LST in Mymensingh, Bangladesh. Their study found that urban expansion over the past two decades resulted in a loss of vegetation and water resources and an increase in surface temperature by approximately 8°C. Gohainet al. [14] evaluated LULC and LST variations in Pune city from 1990 to 2019, concluding that rapid urban development contributed to increased summer temperatures and decreased winter temperatures. These findings are instrumental for urban planners in making informed decisions. In addition, Tan et al. [15] investigated LULC changes in the Dongting Lake region of China, showing that economic development-induced land changes led to increased LST; built-up areas had higher surface temperatures than water bodies and forests, and the reduction of water surfaces, following the construction of the Three Gorges Dam, led to a 3.5°C increase in winter temperatures.

Remote sensing (RS) techniques have been widely used to assess changes in land use/land cover (LULC) and land surface temperature (LST) in recent years through Landsat imagery [16]. RS offers several advantages, including accessibility to remote areas, provision of otherwise unattainable data, cost-effectiveness, and reduced need for fieldwork. Therefore, many researchers have utilized Landsat and MODIS data to estimate annual changes in LULC and LST. In contrast, traditional field-based studies are time-consuming, expensive, and often unsuitable for large-scale assessments [17]. LST variations are influenced by factors such as changes in land use, seasonal rainfall, climatic conditions, and socio-economic developments [18]. Alterations in land cover patterns are mainly driven by human activities [19], including wildfires [20] and deforestation [21], which contribute to global warming and soil erosion. Geostationary satellites, with their capability to provide data every 30 minutes, offer a unique resource for monitoring daily Earth surface changes.

The Hamoun wetland, situated in southeastern Iran near the border with Afghanistan, is of high ecological and socioeconomic importance. Due to frequent droughts, upstream water management, and land use pressures, the area has experienced significant environmental degradation in recent decades. Understanding the drivers and impacts of such changes is essential for sustainable management. The primary aim of the present study is to analyze and evaluate the temporal trends of LULC changes and their impact on land surface temperature (LST) in the Hamoun wetland during the years 1990, 2000, 2010, and 2020. Using satellite data and remote sensing techniques, this research seeks to identify spatial-temporal patterns of change to support sustainable environmental resource management in the region

2. Materials and methods

2.1. Study area

The Hamoun Wetland is located between 60 degrees 39 minutes and 61 degrees 35 minutes Eastern longitude and 31 degrees 15 minutes and 31 degrees 32 minutes Northern latitude. This wetland consists of lakes, ponds, and marshes, with its surface area constantly fluctuating and changing. The maximum area of Hamoun Wetland is approximately 5700 square kilometers, of which 3820 square kilometers are located in Iran [22]. The depth range of the wetland varies between 1 to 7 meters. Hamoun contains mostly permanent, freshwater lakes. This region is situated in a dry and desert climate of Iran, with an annual rainfall of approximately 61 mm [23]. Geologically, it is part of the Helmand basin, a large portion of which is located in Afghanistan. Fig. 1 shows the location of the study area.

2.2. Data used

To assess the trend of land use/land cover changes, Landsat 8 satellite images were obtained from the Earth Explorer website (earthexplorer.usgs.gov) and were prepared for necessary preprocessing and processing. The details of these images are provided in Table 1.

For preparing the land use map on the acquired images, radiometric correction and atmospheric correction were performed [24]. After applying the necessary preprocessing steps, the land use classification map for the Hamoun region for the years 1990, 2000, 2010, and 2020 was created in the GIS environment. Then, supervised classification using the CART model was applied. This method is recognized as a powerful yet simple tool [25, 26]. In fact, the analysis of complex data requires analytical methods that can control nonlinear relationships and interactions. CART is an invariant regression method. The advantages of using the CART method are:

1. The use of a wide variety of variables, including categorical data, survival data, and ordinal data,
2. Simplicity and robustness,
3. Ease of decomposition, analysis, and interpretation, and
4. The ability to handle missing data.

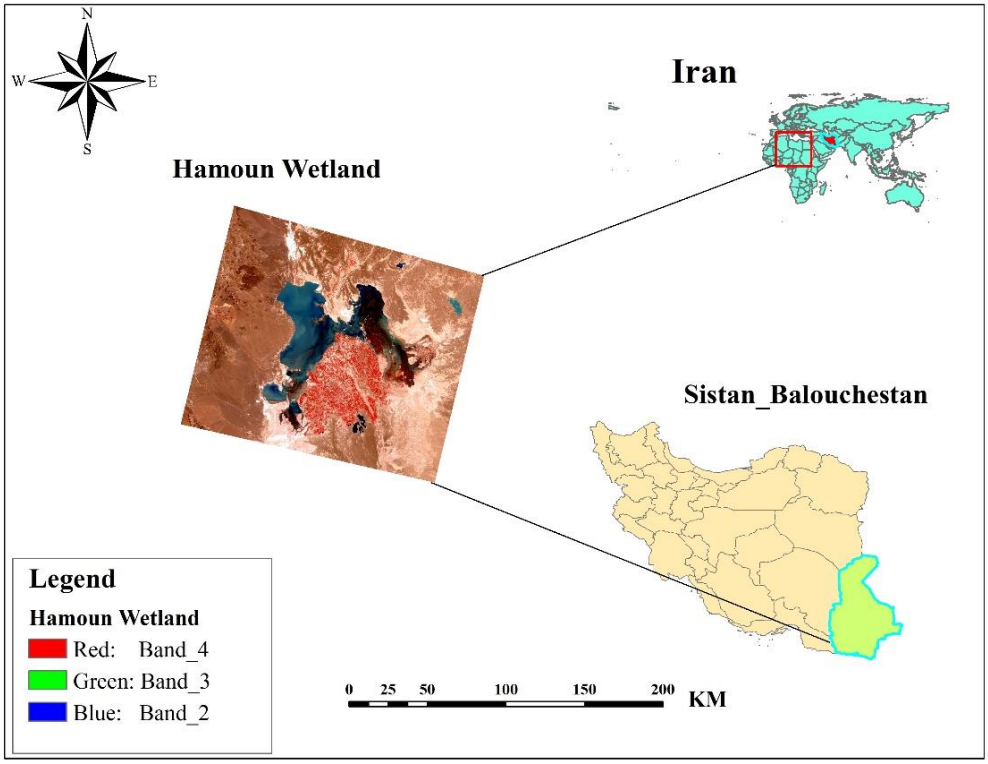

Fig. 1. Location of Hamoun wetland.

Table 1. Specifications of the satellite images used.

Gregorian	Row/Path	Satellite	Sensor	Spatial Resolution (Meters)
1990	39/157	Landsat 5	TM	30
2000	39/157	Landsat 5	TM	30
2010	39/157	Landsat 5	TM	30
2020	39/157	Landsat 5	TM	30

Therefore, this method can serve as an alternative to traditional methods such as logistic regression, multiple regression, and logarithmic-linear models. The CART method was specifically chosen over other classification algorithms such as Support Vector Machines (SVM) and Random Forest due to its interpretability, lower computational cost, and strong performance on datasets with noise and limited sample sizes. This makes CART particularly suitable for analyzing land use changes in complex and ecologically sensitive regions like the Hamoun wetland. The images for land use in the years 1990, 2000, 2010, and 2020 were classified into six land classes, including residential and built-up areas, agricultural land, pastures and low-cover areas, barren land, reed beds, and water bodies. The details of each of these land uses are provided in Table 2. Additionally, NDVI indices were used to estimate vegetation cover, as shown in Eq. 1 [27, 28].

$$\mathrm{NDVI} = \frac{\mathrm{NIR}-\mathrm{R}}{\mathrm{NIR}+\mathrm{R}} \quad (1)$$

$$\mathrm{NDWI} = \frac{\mathrm{B3}-\mathrm{B5}}{\mathrm{B3}+\mathrm{B5}} \quad (2)$$

Table 2. Details of land uses used in the study.

Land Use Land Changes	Explanations
Residential and human-made areas	Residential, commercial areas, transportation networks such as roads and rail networks
Agricultural lands	Dense vegetation cover, agricultural, orchard, and cultivated lands
Pastures and lands with sparse vegetation	Pastures, lands with sparse vegetation
Wastelands	Saline lands and areas without vegetation cover
Water vegetation	Vegetation cover in waterbeds
Waterbeds	Lakes, dams, semi-deep wells

In Eq. 1, NIR represents the near-infrared band, R is the red band, and SWR refers to the shortwave infrared band. The values of these indices typically range between −1 and +1, where values closer to +1 indicate higher index levels. NDVI values range from −1 to +1 regardless of brightness, reflectance, or DN used as input. Generally, negative NDVI values correspond to water bodies, values close to zero are associated with rocks, sands, or concrete surfaces, and positive values indicate vegetative cover, including

plants, shrubs, grasses, and forests. Moreover, many researchers have utilized the Normalized Difference Vegetation Index (NDVI) to detect land cover changes, as it effectively distinguishes vegetation (positive values), bare soil (values near zero), and water bodies (negative values).

In Eq. 2, B3 is the green band, which reflects visible light and is useful for detecting water; B5 is the near-infrared (NIR) band, which is strongly absorbed by water. The NDWI value ranges from -1 to +1, and values greater than zero typically indicate the presence of water bodies.

After the completion of the land use maps and classification of the land uses, the accuracy of these land uses was evaluated. An error matrix was created to assess the accuracy of the generated land uses compared to the ground reality. In this matrix, the producer's accuracy, user's accuracy, overall accuracy, and Kappa coefficient were calculated [29]. The Kappa index considers the incorrectly classified pixels and calculates the classification accuracy relative to a completely random classification. The Kappa index was calculated using Eq. 3.

$$Kappa = \frac{P_0 - P_c}{1 - P_c} \quad (3)$$

In this equation, P_0 represents the observed accuracy, and Pc represents the expected agreement.

2.3. Land use and land cover changes

In this study, land use and land cover changes were examined by analyzing the changes in classified classes during the years 1990, 2000, 2010, and 2020. Accordingly, the changes in various classes were calculated in terms of square kilometers and percentages.

$$Percentage\ of\ Changes = \left(\frac{\mathrm{A}-\mathrm{B}}{\mathrm{B}}\right) * 100 \quad (4)$$

$$Rate\ of\ changes\ (kilometers\ per\ year) = \left(\frac{\mathrm{A}-\mathrm{B}}{C}\right) * 100 \quad (5)$$

In this equation, A represents the area of land use and land cover in the second year, and B represents the area of land use and land cover in the first year. Subsequently, land use changes during the years 1990, 2000, 2010, and 2020 were obtained.

2.4. Land surface temperature data

In climate change studies, one of the most significant indicators reflecting the impacts of climate change is the variation in land surface temperature. Therefore, in this research, to assess the impact of land use on changes in land surface temperature, data from the MODIS satellite under the product name MOD11A2 with a spatial resolution of one kilometer and 8-day temporal intervals for the years 1990, 2000, 2010, and 2020 were extracted from the Earth Data website. The MODIS satellite includes two sensors, Aqua and Terra, which provide long-term datasets with similar land physical parameters for climate and global change studies [30].

2.5. Palmer drought severity index (PDSI)

The Palmer Drought Severity Index (PDSI) is another widely used drought index for monitoring hydrological droughts and is increasingly applied to assess the impacts of climate change [31, 32]. This index is calculated based on temperature, precipitation, and soil moisture data [33]. Table 3 shows the range of PDSI values, which typically vary between -4 and +4 [34].

Table 3. Palmer Drought Severity Index (PDSI) classification.

Drought Range	Drought Classification
<-4	Severe Drought
(-4, -3)	Moderate Drought
(-3, -2)	Mild Drought
(-2, -1)	Normal Wetness
(-1, +1)	Slightly Wet
(+1, +2)	Moderately Wet
(+2, +3)	Very Wet
(+3, +4)	Extremely Wet

3. Results

3.1. Land use changes from 1990 to 2020

The results of the study on land use change over 40 years from 1990 to 2020 are presented in Fig. 2 and Table 4. This study showed that residential areas in the years 1990, 2000, 2010, and 2020 were 0.04%, 0.10%, 0.20%, and 0.30%, respectively, indicating an increasing trend over this period. Additionally, barren lands in 2010 and 2020 were 6714.22 km² and 7166.79 km², respectively, and pastures and lands with sparse vegetation had the largest area during these years, with 13460.84 km² and 14471.50

km², respectively. Over these four decades, reed beds had the smallest area, with 4.64%, 3.14%, 2.27%, and 0.38%, respectively. Moreover, water bodies decreased from 2607.17 km² in 1990 to 573.17 km² in 2020.

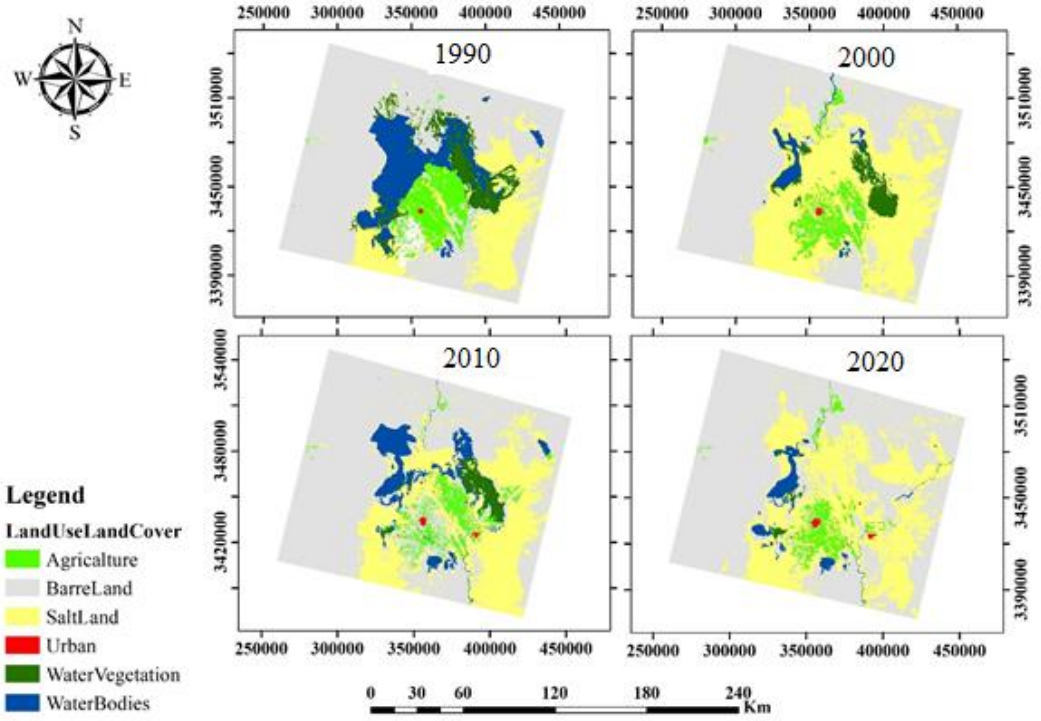

Fig. 2. Land use change map for 1990, 2000, 2010, and 2020 Hamun wetland.

Table 4. Accuracy assessment of land use classes for the years 1990, 2000, 2010, and 2020, Hamun wetland.

	1990				2000				2010				2020			
LULC	Producer Accuracy	User Accuracy	Kappa Coefficient	Overall Accuracy	Producer Accuracy	User Accuracy	Kappa Coefficient	Overall Accuracy	Producer Accuracy	User Accuracy	Kappa Coefficient	Overall Accuracy	Producer Accuracy	User Accuracy	Kappa Coefficient	Overall Accuracy
Agriculture	0.95	0.96			0.99	0.95			0.97	0.96			1	0.96		
SaltLand	0.95	0.98			0.94	0.99			0.94	0.99			0.92	0.98		
BarreLand	0.97	0.98	0.97	0.96	0.94	0.98	0.97	0.96	0.97	0.97	0.96	0.95	0.92	0.97	0.98	0.98
Urban	1	0.93			1	0.92			1	0.94			1	0.93		
WaterVegetation	0.97	0.97			0.99	0.99			0.97	0.97			1	0.94		
WaterBodies	1	0.97			1	0.96			0.99	0.97			1	0.96		

3.2. Accuracy assessment of Hamun land use classes from 1990 to 2020

The evaluation of the accuracy of the Hamun land use maps over 40 years from 1990 to 2020, as shown in **Table 4**, revealed that the Kappa coefficient was 0.97%, 0.97%, 0.96%, and 0.98% for each year, and the overall accuracy was approximately 96%, 96%, 95%, and 98%, respectively. The results of the accuracy estimation for six land use classes—barren lands, pastures and lands with sparse vegetation, reed beds, agriculture, water bodies, and residential areas in the Hamun Lake basin from 1990 to 2020—indicated that the overall accuracy was above 95% and the Kappa coefficient was above 94%, demonstrating sufficient accuracy in the produced land use maps (Table 4).

In this study, the analysis of land use changes in the study area showed that the percentage of barren lands, residential and human-made areas, pastures, and lands with sparse vegetation increased over the four decades. In contrast, the percentage of agricultural lands, reed beds, and water bodies decreased from 8.56%, 4.64%, and 11.25% in 1990 to 3.53%, 0.38%, and 2.47% in 2020, respectively.

Between 1990 and 2000, a decrease in agricultural lands, pastures, and lands with sparse vegetation, and water bodies was observed. Specifically, barren lands, residential and human-made areas, and reed beds increased by 21.28%, 0.06%, and 9.39%, respectively. Furthermore, between 2000 and 2010, pastures and lands with sparse vegetation, residential and human-made areas, and reed beds were on the rise. However, during this period, agricultural lands, barren lands, and water bodies decreased by -0.88%, -9.19%, and -0.87%, respectively. Between 2010 and 2020, reed beds and water bodies showed a decreasing trend of -3.48% and -1.91%, respectively. On the other hand, agricultural lands, pastures and lands with sparse vegetation, barren lands, and residential

areas increased.

Overall, from 1990 to 2020, the trend in land use changes for pastures and lands with sparse vegetation, barren lands, and residential and human-made areas increased by 3.88%, 14.05%, and 0.16%, respectively, while agricultural lands, reed beds, and water bodies decreased by -5.04%, -8.78%, and -4.27% (Table 5).

Table 5. Rate and percentage of area changes in hamun wetland land uses from 1990 to 2020.

Use Types Land	1990-2000%	2000-2010	2010-2020	1990-2020
Agricultural Land	-3.44	-0.88	-0.72	-5.04
Pastures and Lands with Sparse Vegetation	-7.02	6.75	4.14	3.88
Barren Lands	21.28	-9.19	1.95	14.05
Residential and Human-Made Areas	0.06	0.09	0.00	0.16
Water Vegetation	9.39	4.09	-3..48	-8.78
Water Bodies	-1.50	-0.87	-1.91	-4.27

During the years 2000–1990, out of 100 percent of agricultural lands, 48 percent were converted to pastures and lands with sparse vegetation, and out of 100 percent of water bodies, 68 percent were converted to pastures and lands with sparse vegetation, Moreover, out of 100 percent of reed beds, 51 percent were converted to pastures and lands with sparse vegetation, whereas during the years 2020–2010, out of 100 percent of agricultural lands, 42 percent were converted to pastures and lands with sparse vegetation, out of 100 percent of water bodies, 57 percent were converted to pastures and lands with sparse vegetation, and out of 100 percent of reed beds, 78 percent were converted to barren lands. Additionally, during the years 1990–2020, out of 100 percent of agricultural lands, 50 percent were converted to pastures and lands with sparse vegetation, out of 100 percent of water bodies, 53 percent were converted to pastures and lands with sparse vegetation, and out of 100 percent of reed beds, 50 percent were converted to barren lands and 45 percent to pastures and lands with sparse vegetation (Fig. 3).

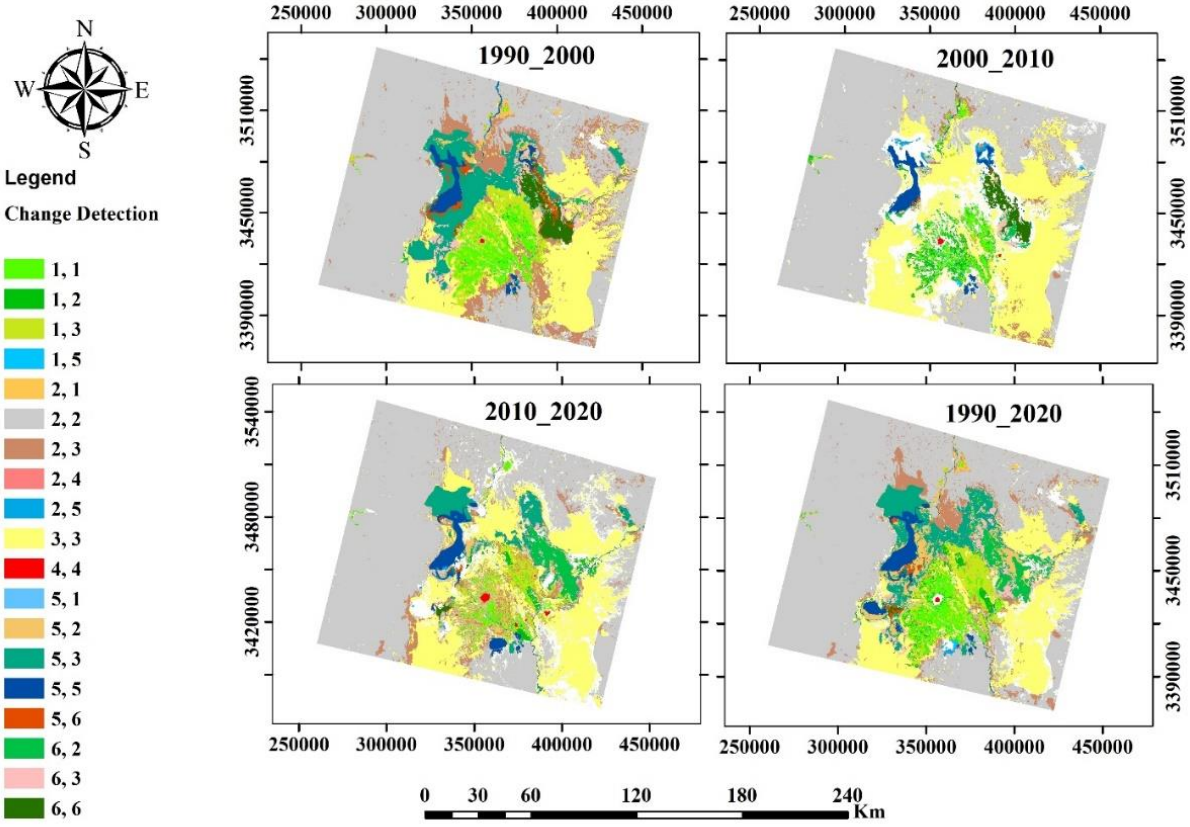

Fig. 3. Rates and percentage areas of land use changes from 1990 to 2020 in the Hamoun wetland.

The results showed that the NDVI decreased from 1990 to 2010 due to water scarcity and the expansion of barren lands (Fig. 4).

The results also indicate that the water bodies had the highest extent in 1990, but showed a decreasing trend in 2000, 2010, and 2020 due to the onset of drought (Fig. 5).

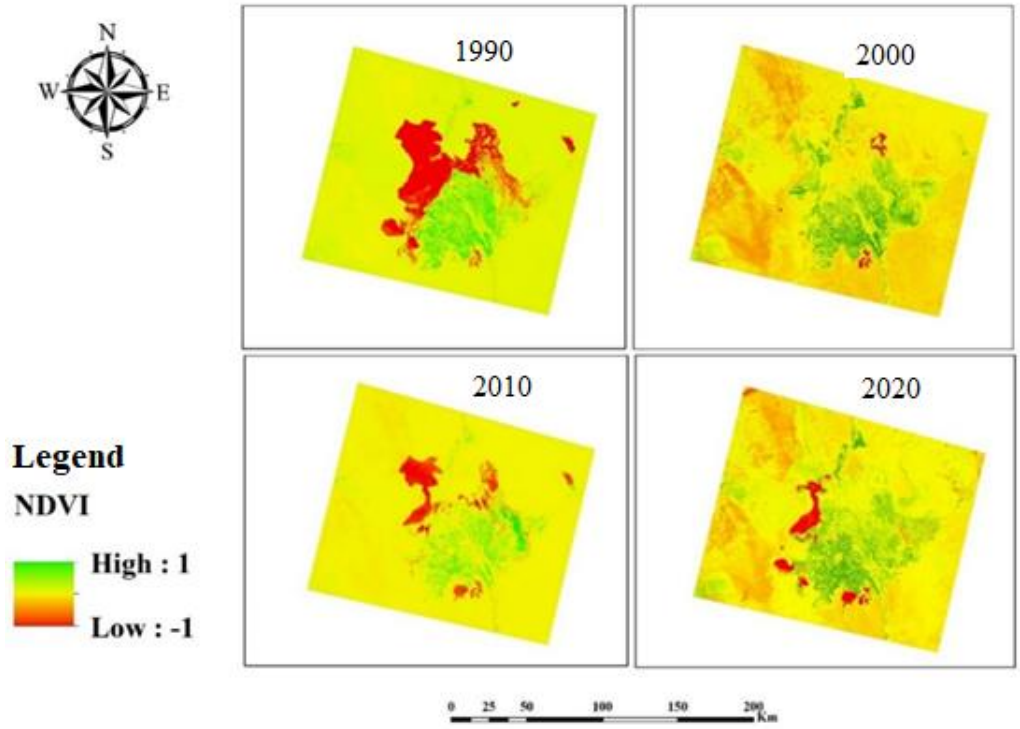

Fig. 4. Normalized difference Vegetation Index (NDVI) in the years 1990, 2000, 2010, and 2020 in the Hamoun wetland.

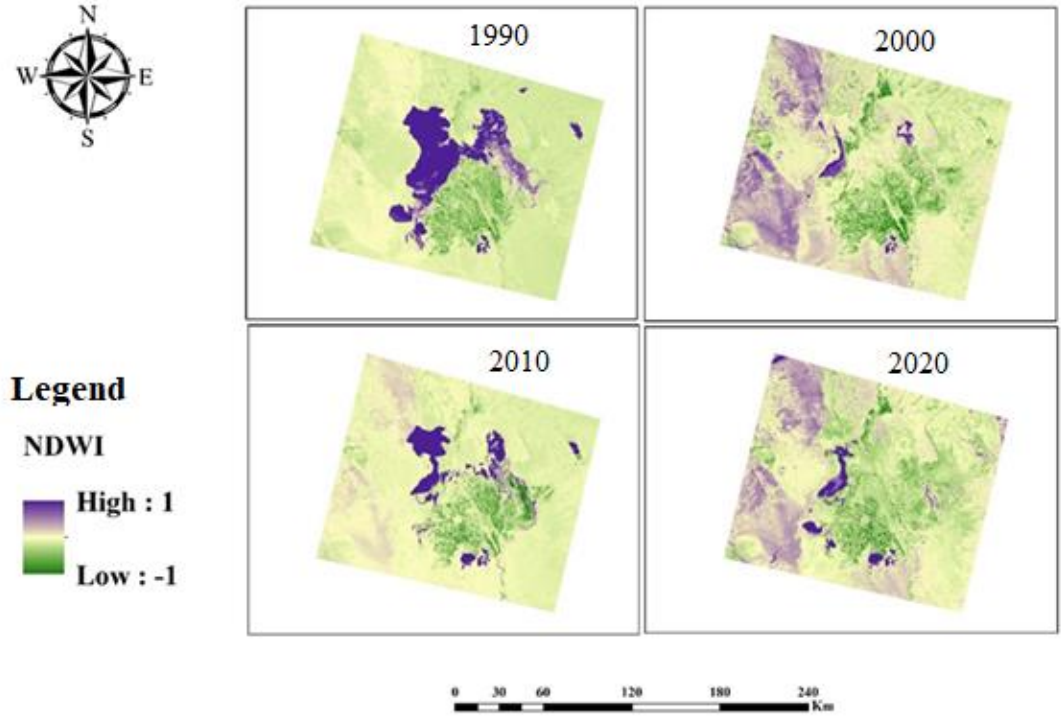

Fig. 5. Water Body index in the years 1990, 2000, 2010, and 2020 in the Hamoun wetland.

3.3. Land surface temperature (LST)

The main issue for government managers in the contemporary context of global warming is the increase in LST in urban areas [35]. As shown in Fig. 6, the highest average daytime temperature in 2000 (Fig. 6(a)) corresponds to barren lands and reed beds, while the lowest average temperature is observed in water bodies. In the same year (2000), the highest average nighttime temperature (Fig. 6(d)) is found in barren and urban areas, and the lowest is in reed beds. In 2010 (Fig. 6(c)), the highest and lowest average daytime temperatures are recorded in barren lands and water bodies, respectively. For the same year, the highest nighttime temperature (Fig. 6(e)) is seen in water bodies, while the lowest is in barren lands. In 2020 (Figs. 6(c) and 6(f)), both daytime and nighttime average temperatures across all land cover types show a decreasing trend. The highest average daytime temperature is found in barren lands, while the lowest is in water bodies (Fig. 6(c)). Conversely, the highest nighttime temperature is seen in water bodies and the lowest in rangelands and sparsely vegetated lands (Fig. 6).

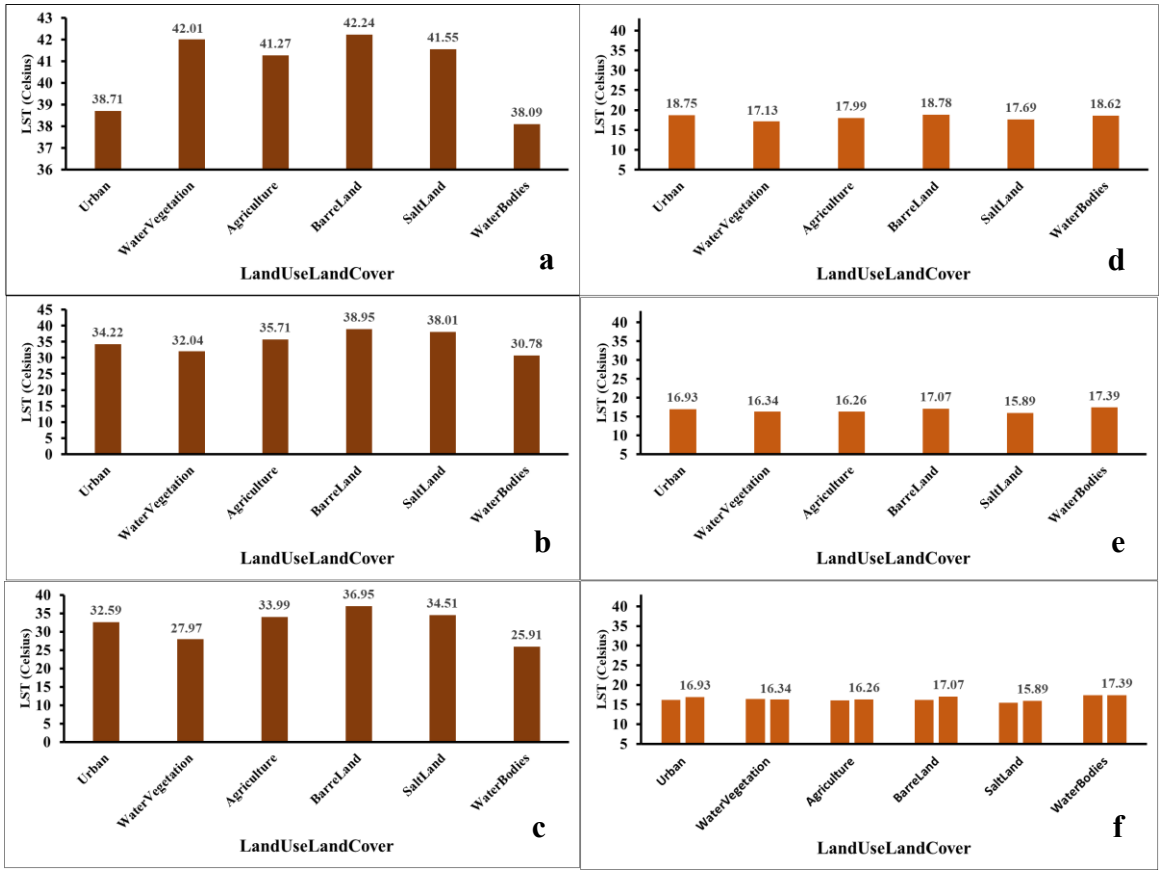

Fig. 6. (a), (b), and (c) Land Surface Day Temperature, (d), (z), and (r) Land Surface Night Temperature in the years 2000, 2010, and 2020 in the Hamoun Wetland.

3.4. Palmer drought severity index

According to the results obtained in Fig. 7, continuous droughts were observed from 1990 to 2020. The results presented in Fig. 8 showed that in 1990, the highest percentage was moderate wet conditions (88.04%), while the lowest percentage was normal drought (11.96%). Additionally, in 2000, the highest amount of drought, including severe, moderate, and mild drought, was observed, with percentages of 0.14%, 36.93%, and 62.93%, respectively. Then, in 2010, moderate drought (34.51%) and mild drought (65.49%) had the highest percentages. Finally, in 2020, four classes were evaluated in the region: moderate wet, mild, very wet, and extremely wet, with the highest percentage being very wet (42.31%), as identified in Fig. 7.

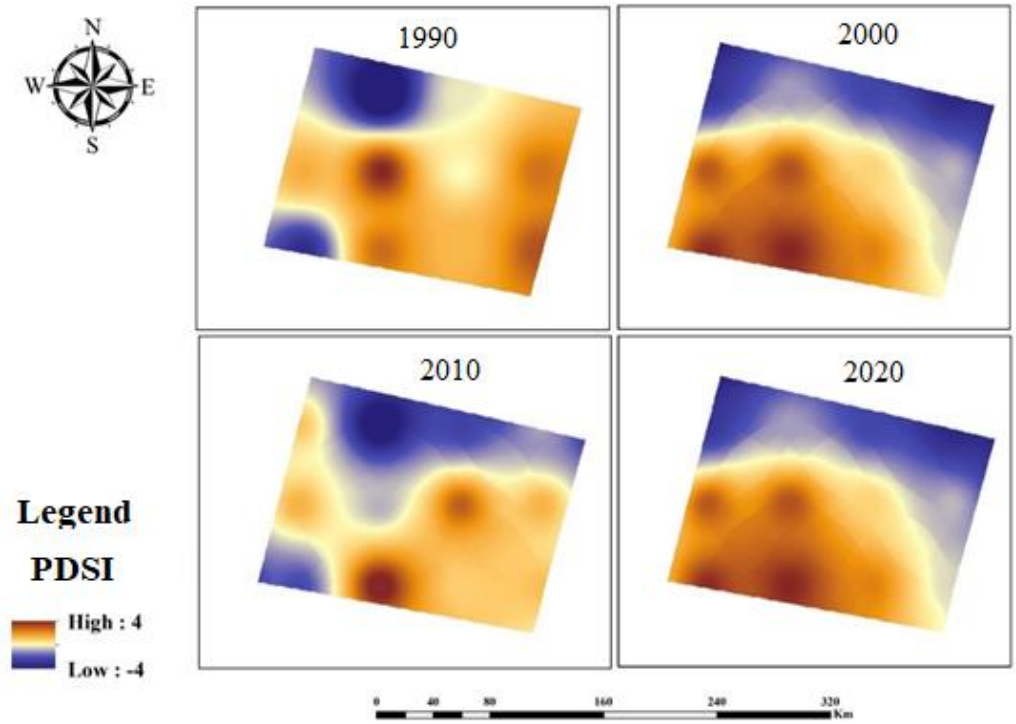

Fig. 7. Palmer drought index for the years 1990, 2000, 2010, and 2020 in Hamoun wetland.

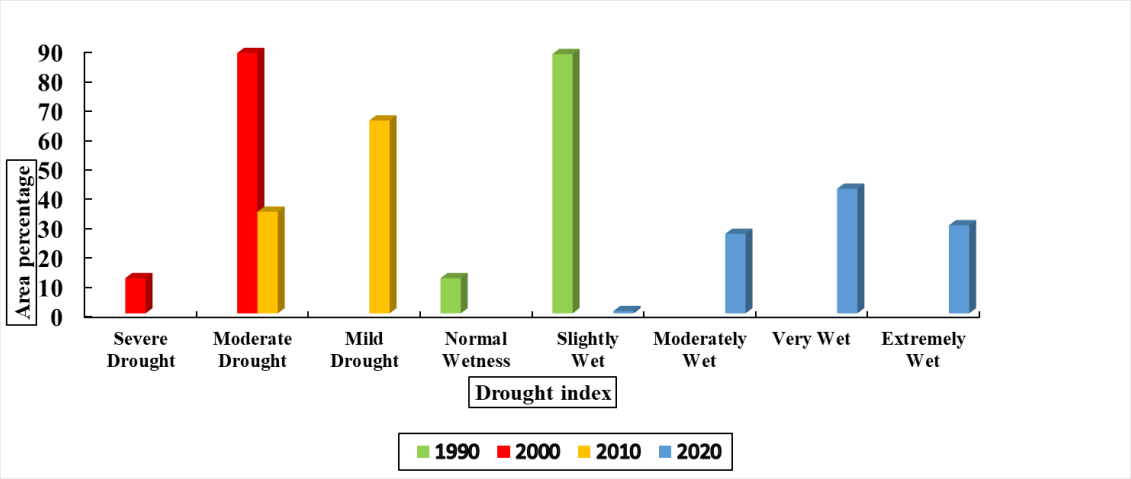

Fig. 8. Palmer drought index for the years 1990, 2000, 2010, and 2020 in Hamoun wetland.

The drought indices in 2000 and 2010 show moderate, normal, and extended droughts. As shown in Fig. 8, a significant drying of the water body occurred in 2000. Additionally, moderate wet conditions were observable in 1990, and more severe wet conditions occurred in 2010. With the land use changes, a decrease in temperature in the studied area was observed, which is due to the droughts that occurred over these four decades.

4. Discussion

The results of the land use change analysis using satellite images in the study area showed that over these forty years, the trend of water bodies, agricultural lands, and reed beds decreased, while barren lands, pastures, areas with sparse vegetation, and cities increased. This aligns with the results of Safari Shad et al. (2000). In other words, over time, with the reduction of water bodies, the amount of agricultural lands and reed beds decreased, but pastures, barren lands, and urban areas increased. Due to the increase in barren lands, conditions suitable for soil erosion potential arise, leading to massive 120-day dust storms blowing from the wetland to the residential areas [36]. On the other hand, Maleki and Koupaei [37] indicated that between 1985 and 2020, in the Hamun wetland, water flowed only 20% of the time, and on average, for less than two months between 1985 and 2020. It also shows that due to repeated droughts and reduced water inflows to Iran, parts of the water bodies have completely dried up. In these years, farmers, livestock herders, fishermen, and wildlife have been harmed [37]. These issues highlight the importance of restoring the Hamun wetland. Furthermore, with the reduction of barren lands, the potential for soil erosion has also decreased. The surface temperature analysis results show a significant decreasing trend from 1990 to 2020, attributed to the ongoing droughts during this period.

The study of climate change trends conducted by Karami et al. [38] indicates a decrease in water reserves. Therefore, the findings of this study show a reduction in water reserves in this wetland due to drought.

The results of the studies by Haji Hosseini et al. [39] regarding land use changes downstream of the Kajaki Dam in Afghanistan showed that the increase in the area under cultivation of agricultural products is one of the reasons for the decrease in the runoff entering Iran from the Helmand River, leading to a reduction in the cultivated area and an increase in barren lands.

According to these results, there is a direct relationship between land use changes and the lives of stakeholders. Sharif Nia et al. [40] examined the situation of stakeholder groups (livestock herders, farmers, etc.) regarding their connection to the wetland and found that stakeholders considered the restoration of this wetland essential for their livelihoods and it has a significant impact on the local population's lives.

5. Conclusion

The present study was conducted to examine the trend of land use changes and their effect on land surface temperature (LST) in the Hamoun wetland from 1990 to 2020 using Geographic Information Systems (GIS) and remote sensing. Landsat 5 and 8 images were used for analyzing the land use changes. Additionally, annual temperature data were used to examine temperature changes, and the Palmer Drought Severity Index (PDSI) was utilized to assess drought conditions.

Overall, the land use changes in the Hamoun wetland were analyzed over four decades using the supervised classification method (CART), which showed a high Kappa coefficient of over 94%. The results of the current study indicate that the area of water bodies has decreased, leading to a reduction in agricultural lands and reed beds. As a result of these changes, pastures, areas with sparse vegetation, barren lands, and urban areas have shown an increasing trend. Furthermore, land surface temperature has shown a significant decreasing trend due to the occurrence of droughts over these decades. In general, the area of water bodies, reed beds, agricultural lands, and the average land surface temperature have decreased.

Thus, by using Landsat 5 and 8 images, the trend of land use changes can be effectively assessed, and by using MODIS images, the changes in land surface temperature can be accurately estimated. The Hamoun wetland is considered one of the important areas of the country from social, economic, and environmental perspectives. The shortage of incoming water resources and water bodies,

along with the drying up of the wetland, has led to the migration of many people from the border areas. Afghanistan's activities upstream of the Helmand River have had an impact on the water resources entering Iran's basin. During drought periods, due to the lack of water resources and the increase in barren lands, very few farmers and livestock herders have been able to use the area.

Due to the water shortage in the studied region, the conditions have become very challenging, especially for stakeholders in agriculture, which has created migration conditions for these stakeholders. According to the presented results, the changes in the extent of water bodies have affected other land uses. Therefore, the preservation and restoration of the Hamoun wetland and the management of water resources are crucial for the living conditions in the region.

Statements & declarations

Author Contributions

Mozhgan Yarahmadi: Conceptualization, Investigation, Methodology, Formal analysis, Resources, Writing - Original Draft, Writing - Review & Editing.

Hadi Eskandari Damaneh: Investigation, Visualization, Validation, Formal analysis, Resources, Writing - Original Draft, Writing - Review & Editing.

Shahram Khalighi Sigaroodi: Conceptualization, Methodology, Formal analysis, Project administration, Supervision, Writing - Review & Editing.

Funding

The authors received no financial support for the research, authorship, and/or publication of this article.

Declarations

The authors declare no conflict of interes.

Data availability

The data presented in this study will be available on interested request from the corresponding author.

References

[1] FAO/UNEP. Terminology for integrated resources planning and management. Rome (Italy): Food and Agriculture Organization/United Nations Environment Programme; 1999.

[2] Mann, M. E., Zhang, Z., Rutherford, S., Bradley, R. S., Hughes, M. K., Shindell, D., Ammann, C., Faluvegi, G., Ni, F. Global Signatures and Dynamical Origins of the Little Ice Age and Medieval Climate Anomaly. Science, 2009; 326 (5957): 1256–1260. doi:10.1126/science.1177303.

[3] Ramachandra, T. V., Aithal, B. H., D, D. S. Land Surface Temperature Analysis in an Urbanising Landscape through Multi- Resolution Data. Research & Reviews: Journal of Space Science & Technology, 2012; 1 (1): 1–10.

[4] Sahoo, S., Dhar, A., Kar, A. Environmental Vulnerability Assessment Using Grey Analytic Hierarchy Process Based Model. Environmental Impact Assessment Review, 2016; 56: 145–154. doi:10.1016/j.eiar.2015.10.002.

[5] Guo, Z., Wang, S. D., Cheng, M. M., Shu, Y. Assess the Effect of Different Degrees of Urbanization on Land Surface Temperature Using Remote Sensing Images. Procedia Environmental Sciences, 2012; 13: 935–942. doi:10.1016/j.proenv.2012.01.087.

[6] Kidder, S. Q., Wu, H. T. A Multispectral Study of the St. Louis Area under Snow-Covered Conditions Using NOAA-7 AVHRR Data. Remote Sensing of Environment, 1987; 22 (2): 159–172. doi:10.1016/0034-4257(87)90056-3.

[7] Balling, R. C., Brazel, S. W. High-Resolution Surface Temperature Patterns in a Complex Urban Terrain. Photogrammetric Engineering & Remote Sensing, 1988; 54 (9): 1289–1293.

[8] Srivastava, P. K., Majumdar, T. J., Bhattacharya, A. K. Study of Land Surface Temperature and Spectral Emissivity Using Multi-Sensor Satellite Data. Journal of Earth System Science, 2010; 119 (1): 67–74. doi:10.1007/s12040-010-0002-0.

[9] Zhang, F., Tiyip, T., Kung, H., Johnson, V. C., Maimaitiyiming, M., Zhou, M., Wang, J. Dynamics of Land Surface Temperature (LST) in Response to Land Use and Land Cover (LULC) Changes in the Weigan and Kuqa River Oasis, Xinjiang, China. Arabian Journal of Geosciences, 2016; 9 (7). doi:10.1007/s12517-016-2521-8.

[10] Zhao, Q., Haseeb, M., Wang, X., Zheng, X., Tahir, Z., Ghafoor, S., Mubbin, M., Kumar, R. P., Purohit, S., Soufan, W., Almutairi, K. F. Evaluation of Land Use Land Cover Changes in Response to Land Surface Temperature With Satellite Indices and Remote Sensing Data. Rangeland Ecology and Management, 2024; 96: 183–196. doi:10.1016/j.rama.2024.07.003.

[11] Saleem, H., Ahmed, R., Mushtaq, S., Saleem, S., Rajesh, M. Remote Sensing-Based Analysis of Land Use, Land Cover, and Land Surface Temperature Changes in Jammu District, India. International Journal of River Basin Management, 2024; 1–16.

doi:10.1080/15715124.2024.2327493.

[12] Hussain, S., Karuppannan, S. Land Use/Land Cover Changes and Their Impact on Land Surface Temperature Using Remote Sensing Technique in District Khanewal, Punjab Pakistan. Geology, Ecology, and Landscapes, 2023; 7 (1): 46–58. doi:10.1080/24749508.2021.1923272.

[13] Al Rakib, A., Akter, K. S., Rahman, M. N., Arpi, S., Kafy, A. A. Analyzing the pattern of land use land cover change and its impact on land surface temperature: a remote sensing approach in Mymensingh, Bangladesh. In: Proceedings of the 1st International Student Research Conference - 2020; 2020 Apr; Dhaka, Bangladesh.

[14] Gohain, K. J., Mohammad, P., Goswami, A. Assessing the impact of land use land cover changes on land surface temperature over Pune city, India. Quaternary International, 2021; 575: 259–269. doi:10.1016/j.quaint.2020.04.052.

[15] Tan, J., Yu, D., Li, Q., Tan, X., Zhou, W. Spatial Relationship between Land-Use/Land-Cover Change and Land Surface Temperature in the Dongting Lake Area, China. Scientific Reports, 2020; 10 (1): 9245. doi:10.1038/s41598-020-66168-6.

[16] Parastatidis, D., Mitraka, Z., Chrysoulakis, N., Abrams, M. Online Global Land Surface Temperature Estimation from Landsat. Remote Sensing, 2017; 9 (12): 1208. doi:10.3390/rs9121208.

[17] Dissanayake, D., Morimoto, T., Ranagalage, M. Accessing the Soil Erosion Rate Based on RUSLE Model for Sustainable Land Use Management: A Case Study of the Kotmale Watershed, Sri Lanka. Modeling Earth Systems and Environment, 2019; 5 (1): 291–306. doi:10.1007/s40808-018-0534-x.

[18] Jiang, J., Tian, G. Analysis of the Impact of Land Use/Land Cover Change on Land Surface Temperature with Remote Sensing. Procedia Environmental Sciences, 2010; 2: 571–575. doi:10.1016/j.proenv.2010.10.062.

[19] Yue, W., Xu, J., Tan, W., Xu, L. The Relationship between Land Surface Temperature and NDVI with Remote Sensing: Application to Shanghai Landsat 7 ETM+ Data. International Journal of Remote Sensing, 2007; 28 (15): 3205–3226. doi:10.1080/01431160500306906.

[20] Nunes, M. C. S., Vasconcelos, M. J., Pereira, J. M. C., Dasgupta, N., Alldredge, R. J., Rego, F. C. Land Cover Type and Fire in Portugal: Do Fires Burn Land Cover Selectively? Landscape Ecology, 2005; 20 (6): 661–673. doi:10.1007/s10980-005-0070-8.

[21] Huang, S., Siegert, F. Land Cover Classification Optimized to Detect Areas at Risk of Desertification in North China Based on SPOT VEGETATION Imagery. Journal of Arid Environments, 2006; 67 (2): 308–327. doi:10.1016/j.jaridenv.2006.02.016.

[22] Dehghani, T., Koolivand, I., Mehdizadeh, S., Ahmadpari, H., Zolfagharan, A., Mohamadi, E. Monitoring land-use changes using remote sensing, ENVI and ArcGIS software in Hamoun Wetlands. In: Proceedings of the 3rd International and 6th National Conference on Conservation of Natural Resources and Environment; 2022 Sep 12–13; Ardabil, Iran.

[23] Kharazmi, R., Abdollahi, A. A., Rahdari, M. R., Karkon varnosfaderani, M. Monitoring Land Use Change and its Impacts on Land Degradation and Desertification Trend Using Landsat Satellite Images (Case study: East of Iran, Hamoon Wetland). Journal of Arid Regions Geographic Studies, 2022; 7(25): 64-75.

[24] Eskandari Damaneh, H., Zehtabian, G. R., Khosravi, H., Azareh, A. Investigation and Analysis of Temporal and Spatial Relationship between Meteorological and Hydrological Drought in Tehran Province. Scientific- Research Quarterly of Geographical Data (SEPEHR), 2016; 24(96): 113-120. doi:10.22131/sepehr.2016.18947.

[25] Biro, K., Pradhan, B., Buchroithner, M., Makeschin, F. Land Use/Land Cover Change Analysis And Its Impact On Soil Properties In The Northern Part Of Gadarif Region, Sudan. Land Degradation and Development, 2013; 24 (1): 90–102. doi:10.1002/ldr.1116.

[26] Yousefi J. Image binarization using the Otsu thresholding algorithm. Ontario (Canada): University of Guelph; 2011.

[27] Tucker, C. J., Justice, C. O., Prince, S. D. Monitoring the Grasslands of the Sahel 1984-1985. International Journal of Remote Sensing, 1986; 7 (11): 1984–1985. doi:10.1080/01431168608948954.

[28] Gao, B. C. NDWI - A Normalized Difference Water Index for Remote Sensing of Vegetation Liquid Water from Space. Remote Sensing of Environment, 1996; 58 (3): 257–266. doi:10.1016/S0034-4257(96)00067-3.

[29] Kafy, A. A., Naim, M. N. H., Subramanyam, G., Faisal, A. Al, Ahmed, N. U., Rakib, A. Al, Kona, M. A., Sattar, G. S. Cellular Automata Approach in Dynamic Modelling of Land Cover Changes Using RapidEye Images in Dhaka, Bangladesh. Environmental Challenges, 2021; 4: 100084. doi:10.1016/j.envc.2021.100084.

[30] Salomonson, V. V, Guenther, B., Masuoka, E. A summary of the status of the EOS Terra Mission Moderate Resolution Imaging Spectroradiometer (MODIS) and attendant data product development after one year of on-orbit performance. In: Proceedings of the International Geoscience and Remote Sensing Symposium (IGARSS); 2001 Jul 9–13; Sydney, Australia. doi:10.1109/igarss.2001.976790.

[31] Mika, J., Horváth, S., Makra, L., Dunkel, Z. The Palmer Drought Severity Index (PDSI) as an Indicator of Soil Moisture. Physics and Chemistry of the Earth, 2005; 30 (1-3 SPEC. ISS.): 223–230. doi:10.1016/j.pce.2004.08.036.

[32] Zhai, J., Su, B., Krysanova, V., Vetter, T., Gao, C., Jiang, T. Spatial Variation and Trends in PDSI and SPI Indices and Their Relation to Streamflow in 10 Large Regions of China. Journal of Climate, 2010; 23 (3): 649–663. doi:10.1175/2009JCLI2968.1.

[33] Barichivich, J., Osborn, T., Harris, I., van der Schrier, G., & Jones, P. (2021). Monitoring global drought using the self-calibrating Palmer Drought Severity Index [in" State of the Climate in 2020" eds. Dunn RJH, Aldred F, Gobron N, Miller JB & Willett KM]. Bulletin of the American Meteorological Society, 102(8), S68-S70. doi: 10.1175/BAMS-D-21-0098.1.

[34] Zheng, Z., Jin, L., Li, J., Chen, J., Zhang, X., Wang, Z. Moisture Variation Inferred from Tree Rings in North Central China and Its Links with the Remote Oceans. Scientific Reports, 2021; 11 (1): 16463. doi:10.1038/s41598-021-93841-1.

[35] Dhar, R. B., Chakraborty, S., Chattopadhyay, R., Sikdar, P. K. Impact of Land-Use/Land-Cover Change on Land Surface Temperature Using Satellite Data: A Case Study of Rajarhat Block, North 24-Parganas District, West Bengal. Journal of the Indian Society of Remote Sensing, 2019; 47 (2): 331–348. doi:10.1007/s12524-019-00939-1.

[36] Miri, A., Ahmadi, H., Ekhtesasi, M. R., Panjehkeh, N., Ghanbari, A. Environmental and Socio-Economic Impacts of Dust Storms in Sistan Region, Iran. International Journal of Environmental Studies, 2009; 66 (3): 343–355. doi:10.1080/00207230902720170.

[37] Maleki, S., Koupaei, S. S., Soffianian, A., Saatchi, S., Pourmanafi, S., Rahdari, V. Human and Climate Effects on the Hamoun Wetlands. Weather, Climate, and Society, 2019; 11 (3): 609–622. doi:10.1175/WCAS-D-18-0070.1.

[38] Karami, R., Salman Mahini, A., Ghobani Nasrabadi, H., Khalil Evaluation of Climate Change in the Hamun International Wetland Basin Using the LARS-WG6 Model. Natural Environmental Hazards, 11 (31): 107–122.

[39] Haji Hosseini, H., Shigan, M., Morid, V., Alireza Study of Land Use Changes Downstream of the Kajaki Dam in the Helmand River Basin, Afghanistan, Using the Maximum Likelihood Classifier. Decision Trees, and Support Vector Machines. Remote Sensing and GIS Journal of Iran, 5 (4).

[40] Sharif Nia, H., Pahlevan Sharif, S., Yaghoobzadeh, A., Yeoh, K. K., Goudarzian, A. H., Soleimani, M. A., Jamali, S. Effect of acupressure on pain in Iranian leukemia patients: A randomized controlled trial study. International Journal of Nursing Practice, 2017; 23(2): e12513. doi:10.1111/ijn.12513.